Long-Chain Polyprenols Promote Spore Wall Formation in *Saccharomyces cerevisiae*

Reuben Hoffmann,* Kariona Grabińska,† Ziqiang Guan,‡ William C. Sessa,† and Aaron M. Neiman*,1

*Department of Biochemistry and Cell Biology, Stony Brook University, New York 11794-5215, †Department of Pharmacology, Yale School of Medicine, New Haven, Connecticut 06520-8066, and ‡Department of Biochemistry, Duke University School of Medicine, Durham, North Carolina 27710

ORCID ID: 0000-0002-6600-6996 (A.M.N.)

ABSTRACT Dolichols are isoprenoid lipids of varying length that act as sugar carriers in glycosylation reactions in the endoplasmic reticulum. In *Saccharomyces cerevisiae*, there are two *cis*-prenyltransferases that synthesize polyprenol—an essential precursor to dolichol. These enzymes are heterodimers composed of Nus1 and either Rer2 or Srt1. Rer2-Nus1 and Srt1-Nus1 can both generate dolichol in vegetative cells, but *srt1*Δ cells grow normally while *rer2*Δ grows very slowly, indicating that Rer2-Nus1 is the primary enzyme used in mitotically dividing cells. In contrast, *SRT1* performs an important function in sporulating cells, where the haploid genomes created by meiosis are packaged into spores. The spore wall is a multilaminar structure and *SRT1* is required for the generation of the outer chitosan and dityrosine layers of the spore wall. Srt1 specifically localizes to lipid droplets associated with spore walls, and, during sporulation there is an *SRT1*-dependent increase in long-chain polyprenols and dolichols in these lipid droplets. Synthesis of chitin by Chs3, the chitin synthase responsible for chitosan layer formation, is dependent on the *cis*-prenyltransferase activity of Srt1, indicating that polyprenols are necessary to coordinate assembly of the spore wall layers. This work shows that a developmentally regulated *cis*-prenyltransferase can produce polyprenols that function in cellular processes besides protein glycosylation.

KEYWORDS lipid droplet; dolichol; *cis*-prenyltransferase; Chs3; chitosan; Srt1; sporulation; yeast

DOLICHOLS and polyprenols are polyisoprenoid lipids found in all cellular organisms. Their best understood function is as sugar carriers in glycosylation reactions (Abu-Qarn *et al.* 2008). In eukaryotic cells, dolichol phosphate acts as a sugar carrier for N- and O-linked glycosylation as well as glycosylphosphatidylinositol-anchor synthesis in the endoplasmic reticulum (ER) (Burda and Aebi 1999; Loibl and Strahl 2013; Grabińska *et al.* 2016). Polyprenols and dolichols are also found in other cellular membranes besides the ER, but their function in other organelles is unclear.

Polyisoprenoids are formed by the action of *cis*-prenyltransferase enzymes. These enzymes iteratively add 5-carbon isopentenyl groups onto a farnesyl diphosphate "seed" to produce polyprenols—polymers of 14–24 repeating isopentenyl units (Sato *et al.* 2001). Additional enzymes in the ER saturate the

final isopentenyl unit in the polyprenol, creating dolichol (Swiezewska and Danikiewicz 2005). In yeast, the paralogous proteins Rer2 and Srt1 independently associate with a common subunit, Nus1, to generate two different *cis*-prenyltransferase complexes (Sato *et al.* 1999, 2001; Schenk *et al.* 2001; Park *et al.* 2014).

The Srt1-Nus1 and Rer2-Nus1 complexes differ in several ways. First, while Rer2 is localized to both the ER and lipid droplets in vegetative cells (Currie *et al.* 2014), Srt1 is primarily localized to lipid droplets (Sato *et al.* 2001). Second, Rer2 produces shorter polyprenols, averaging 15 isoprene repeat units, while Srt1 produces longer polyprenols, averaging 21 isoprene repeats (Sato *et al.* 2001). Third, in vegetative cells, *SRT1* is expressed primarily in stationary phase, while *RER2* is constitutively expressed (Sato *et al.* 2001). Finally, *rer2*Δ cells show severe growth defects and glycosylation defects (Sato *et al.* 1999), while *srt1*Δ mutants do not. Nonetheless, there is some overlap in function as *srt1*Δ and *rer2*Δ are synthetically lethal and cells deleted for *NUS1* are inviable (Sato *et al.* 1999; Yu *et al.* 2006). Also, *SRT1* overexpression can correct the *rer2*Δ glycosylation defect (Sato *et al.* 1999; Grabińska *et al.* 2005, 2010; Kwon *et al.* 2016).

Rer2-Nus1 is the primary *cis*-prenyltransferase required for dolichol synthesis for protein glycosylation in the ER in vegetative cells, but the role of *SRT1* in cells has been unclear. Although no vegetative phenotypes of *srt1Δ* have been reported, *SRT1* was identified in three different genome-wide screens for mutants that decreased sporulation, raising the possibility that the Srt1 *cis*-prenyltransferase is required for a novel function in spore formation (Deutschbauer *et al.* 2002; Enyenihi and Saunders 2003; Marston *et al.* 2004).

Under conditions of nitrogen starvation and the absence of a fermentable carbon source, diploid cells of *S. cerevisiae* undergo meiosis and sporulation, in which the four haploid nuclei produced by the meiosis are packaged into haploid spores within the mother cell cytoplasm (Neiman 2011). The outside of each spore is composed of a complex wall that provides increased resistance to various external stresses (Coluccio *et al.* 2004, 2008).

Spore formation begins early in Meiosis II (MII), when secretory vesicles coalesce at the cytoplasmic face of each of the four spindle pole bodies, resulting in the formation of four prospore membranes (Neiman 1998). Each prospore membrane grows to engulf a haploid genome and a portion of the cytoplasmic content (Byers 1981). Closure of the prospore membrane separates the spore and mother cell cytoplasm by two lipid bilayers with a lumenal space between them. The spore wall is then constructed within this lumenal space (Lynn and Magee 1970). The lipid bilayer closest to the nucleus goes on to form the spore plasma membrane, while the outer bilayer is lysed during spore wall formation (Coluccio *et al.* 2004).

There are four distinct layers to the spore wall. Going from closest to the spore plasma membrane outward, the layers are composed primarily of (1) mannan (*i.e.*, mannosylated proteins); (2) β-1,3-glucan; (3) chitosan; and (4) dityrosine (Neiman 2011). The inner two layers are similar in composition to the layers of the vegetative cell wall, though they are arranged in reverse order with respect to the plasma membrane (Kreger-Van Rij 1978; Smits *et al.* 2001). The chitosan and dityrosine layers are unique to spores and are essential for increased stress resistance (Briza *et al.* 1988, 1990a,b; Pammer *et al.* 1992).

The spore wall layers are assembled sequentially beginning with the mannan layer (Tachikawa *et al.* 2001). After the deposition of the mannan and glucan layers, the outer membrane bilayer derived from the prospore membrane lyses, placing the glucan layer in contact with the ascal (mother cell) cytoplasm. The outer chitosan layer is then constructed and the wall is finished by the deposition of dityrosine into the wall (Coluccio *et al.* 2004). Proper construction of the dityrosine layer is dependent on prior assembly of the chitosan layer (Coluccio *et al.* 2004).

Chitosan is a polysaccharide composed of β-1,4-glucosamine (Briza *et al.* 1988). The chitosan layer of the spore wall is formed through the sequential action of the chitin synthase, Chs3, and the chitin deacetylases, Cda1 and Cda2 (Pammer *et al.* 1992; Christodoulidou *et al.* 1996, 1999). Chs3 is a polytopic transmembrane protein that produces chitin (β-1,4-N-acetylglucosamine) from uridine diphosphate N-acetylglucosamine (UDP-GlcNAc) in the cytoplasm, and extrudes the polymer through the plasma membrane (Cabib *et al.* 1983; Pammer *et al.* 1992). Cda1 and Cda2 are enzymes localized to the spore wall that deacetylate chitin chains, converting them to chitosan (Christodoulidou *et al.* 1996, 1999; Mishra *et al.* 1997). In the absence of both *CDA1* and *CDA2*, chitin accumulates in the spore wall rather than chitosan (Christodoulidou *et al.* 1999; Lin *et al.* 2013). The chitin is not assembled into a discrete layer, however, and, as a result, both the chitosan and dityrosine layers are absent in a *cda1Δ cda2Δ* mutant.

Chitin deposition is timed with the cell cycle, and the activity of Chs3 is tightly controlled during vegetative growth to allow deposition of chitin at the bud neck (Shaw *et al.* 1991; Pammer *et al.* 1992; Choi *et al.* 1994; Chuang and Schekman 1996; Kozubowski *et al.* 2003). Chs4 (also called Skt5) is a key regulator of Chs3 that controls Chs3 activity in two ways: (1) Chs4 binds Chs3 and allosterically activates the enzyme, and (2) it controls delivery of Chs3 to the bud neck through interactions with transport factors (Ono *et al.* 2000; Kozubowski *et al.* 2003).

In sporulating cells, chitin is synthesized at the spore wall, thereby requiring sporulation-specific regulation of Chs3 localization, which is mediated by the sporulation-specific Sps1 kinase (Iwamoto *et al.* 2005). Yeast cells also contain a sporulation-specific paralog of Chs4 called Shc1 (Sanz *et al.* 2002). Shc1 is capable of the allosteric activation function of Chs4 but not the localization function, as ectopic expression of *SHC1* in vegetative cells activates Chs3 but does not properly localize it to the bud neck. Furthermore, *shc1Δ* diploids display modest spore wall defects, suggesting a role for *SHC1* in Chs3 activation during sporulation.

Another factor involved in formation of the outer spore wall is lipid droplets (Hsu *et al.* 2017). Lipid droplets are organelles composed of a monolayer of phospholipids surrounding a core of neutral lipids (Wang 2015). They act as sites of both lipid storage and metabolism (Kohlwein *et al.* 2013). It is possible for cells to sporulate while lacking lipid droplets that contain either triglycerides or sterol esters, but the absence of any lipid droplets leads to defects in both prospore membrane growth and spore wall assembly (Hsu *et al.* 2017). This result suggests that some lipid droplet factor besides the neutral lipids is essential for proper sporulation.

During sporulation, a subset of lipid droplets associates with the forming prospore membrane (Lin *et al.* 2013). After closure, these droplets remain associated with the outer membrane derived from the prospore membrane. After lysis of the outer membrane the lipid droplets associate with the outer spore wall. These external lipid droplets gradually dwindle both in size and number over the course of spore wall development (Lin *et al.* 2013). Spore wall associated droplets can be distinguished from lipid droplets in the spore cytoplasm by their localization, as well as by specific protein constituents (Ren *et al.* 2014). Several lipid droplet proteins are specifically associated with spore-wall-associated droplets during sporulation (Lam *et al.* 2014; Ren *et al.* 2014). For instance, three paralogous proteins, Lds1, Lds2, and Rrt8 all localize solely to the spore wall lipid droplets and the triple mutant displays defects in formation of the dityrosine layer, indicating a role in spore wall development

(Lin *et al.* 2013). Srt1 and Nus1 both localize to these lipid droplets, suggesting that *cis*-prenyltransferase activity may be present in these spore-wall-associated lipid droplets (Sato *et al.* 2001; Currie *et al.* 2014; Lam *et al.* 2014).

This work shows that *SRT1* functions during sporulation to generate long chain polyisoprenoids in spore-wall-associated lipid droplets. These polyisoprenoids activate the Chs3 chitin synthase to generate the chitin, which is then modified to make the chitosan layer of the spore wall. The finding that polyprenols are required for a developmentally regulated process in sporulating yeast suggests that this interesting type of molecule may have additional roles in other cellular processes beyond glycosylation in the ER.

Materials and Methods

Yeast strains and media

Unless otherwise mentioned, standard yeast media and genetic techniques were used (Rose *et al.* 1990). All the strains used, except AN512, are derived from the SK1 background, and their genotypes are listed in Table 1. Primer sequences are listed in Table 2. AN512 was created by mating the SK1 haploid AN117-4B to an *srt1Δ* mutant in the BY4741 background from the *Saccharomyces* Deletion Collection (Giaever *et al.* 2002), dissecting the resulting diploid, and mating *srt1Δ* segregants with each other. RHY1 and RHY2 (*srt1Δ*) were made by polymerase chain reaction (PCR)-mediated homologous recombination in AN117-16D and S2683 respectively, using the primers CK33 and CK34 with pFA6a-kanMX6 (Bahler *et al.* 1998) as the template. RHY1 and RHY2 were mated to form RHY19 (*srt1Δ/srt1Δ*). RHY27 and RHY28 (*chs4Δ*) were made by PCR-mediated homologous recombination in AN117-4B and AN117-16D respectively, using the primers RHO28 and RHO29 with pFA6a-kanMX6 as the template. RHY27 and RHY28 were mated to form RHY29 (*chs4Δ/chs4Δ*). AN1092 and AN1093 (*shc1Δ*) were made by PCR-mediated homologous recombination in AN117-4B and AN117-16D respectively, using the primers ANO274 and ANO275 with pFA6a-His3MX6 (Longtine *et al.* 1998) as the template. AN1092 and AN1093 (*shc1Δ*) were mated to form AN270 (*shc1Δ/shc1Δ*). RHY23 and RHY24 (*chs4Δ shc1Δ*) were made by PCR-mediated homologous recombination to delete *CHS4* in AN1092 and AN1093 (*shc1Δ*), respectively, using the primers RHO28 and RHO29 with pFA6a-kanMX6 as the template. RHY23 and RHY24 (*chs4Δ shc1Δ*) were mated to form RHY26 (*chs4Δ/chs4Δ shc1Δ/shc1Δ*). RHY37 and RHY38 (*chs4Δ shc1Δ*) were segregants from a cross between AN1092 (*shc1Δ*) and RHY28(*chs4Δ*), and were mated to form RHY39 (*chs4Δ/chs4Δ shc1Δ/shc1Δ*). RHY19-P1 and RHY19-P2 were created by transforming RHY1 and RHY2 (*srt1Δ*) with the integrating vectors pRS306-*SRT1* or pRS306-srt1-D75A, and mating the transformants to produce homozygous diploids.

RHY16 (*CHS3-3xsfGFP/CHS3-3xsfGFP)* was created by tagging *CHS3* at the C-terminus via PCR-mediated homologous recombination in AN117-4B and AN117-16D using a fragment containing three copies of superfolder green fluorescent protein (3xsfGFP) (Jin *et al.* 2017), amplified with the primers YSO1 and YSO2 with pFA6a-3xsfGFP -kanMX6 (a gift from G. Zhao)

as the template. RHY42 (*CHS3-3xsfGFP/CHS3-3xsfGFP*) was created by dissecting RHY16 and crossing segregants with each other. RHY16 was dissected and a segregant crossed with RHY1 (*srt1Δ*) to produce a double heterozygote (*CHS3-3xsfGFP/ CHS3 srt1Δ/SRT1*), which was then dissected and segregants crossed with each other to produce RHY44 (*CHS3-3xsfGFP/ CHS3-3xsfGFP srt1Δ/srt1Δ*). In addition, a *CHS3-3xsfGFP* segregant from RHY16 was crossed with RHY37 (*chs4Δ shc1Δ*) to produce a double heterozygote (*CHS3-3xsfGFP/CHS3 chs4Δ/ CHS4 shc1Δ/SHC1*), which was dissected and segregants were crossed with each other to produce RHY57 (*chs3-3xsfGFP/chs3-3xsfGFP chs4Δ/chs4Δ shc1Δ/shc1Δ*).

Plasmids

pRS306-SRT1 was created by amplifying a 1.7-kb genomic fragment from SK1 strain AN120 (-382 from the start codon to $+276$ bp past the stop codon) containing *SRT1* using the primers CK25 and RHO07. The fragment was engineered to have *Not*I and *Xho*I restriction sites on either end. The *Not*I/ *Xho*I digested fragment was then cloned into *Not*I/*Xho*I digested pRS306 (Sikorski and Hieter 1989). This plasmid was used as the template for site-directed mutagenesis to change codon 75 from GAT to GCT (aspartic acid to alanine: D75A) using the primers RHO08 and RHO09 (Quikchange kit, Stratagene). The resulting 6.1-kb product was digested with *Dpn*I to remove the wild-type plasmid and transformed into *Escherichia coli* (BSJ72). Sequencing of the entire *srt1-D75A* allele from the resulting plasmid, pRS306-srt1-D75A, confirmed the presence of the mutation and the absence of any additional changes. Sequencing was performed by the Stony Brook University DNA Sequencing facility. Both pRS306-SRT1 and pRS306-srt1-D75A were linearized with *Stu*I to target integration to *ura3* in the yeast genome.

To construct a green fluorescent protein (GFP) tagged allele of *SRT1*, a ~7.0-kb *Kpn*I/*Bst*EII fragment containing *SRT1232-1032-GFP* and the pRS316 backbone was isolated from pLN-SRT1-GFP (gift from L. Needleman). A second fragment containing the promoter region (-382) and the first 256 bases of *SRT1* was amplified from pRS306-SRT1 using the primers RHO43 and RHO44, with one end containing overlapping homology adjacent to the *Kpn*I site on pRS316, and the other end overlapping the *Bst*EII site in *SRT1*. These two fragments were then joined together using the Gibson Assembly kit from Invitrogen (GeneArt Seamless Cloning and Assembly Kit, A13288) to make pRS316-*SRT1*-GFP (Gibson *et al.* 2009). The *srt1-D75A-GFP* allele was similarly constructed in pRS316 except that the fragment containing the promoter and the first 256 bases of *SRT1* was amplified from pRS306-srt1-D75A. Both the *SRT1* and *srt1-D75A* open reading frames (ORFs) in these plasmids were sequenced in their entirety to ensure no unexpected mutations were present. pRS426-Spo20$^{51-91}$-RFP and pRS424-Spo20$^{51-91}$-RFP have been previously characterized (Suda *et al.* 2007).

Sporulation

Single colonies of each strain were inoculated into 3 ml of YPD medium and grown on a roller overnight at 30°. These cultures

Table 1 Yeast strains0

Name	Genotype	Reference
AN117-4B	*MATα ura3 leu2 his3ΔSK trp1::hisG arg4-NspI lys2 rme1Δ::LEU2 hoΔ::LYS2*	Neiman *et al.* (2000)
AN117-16D	*MAT**a** ura3 leu2 his3ΔSK trp1::hisG lys2 hoΔ::LYS2*	Neiman *et al.* (2000)
S2683	*MATα ura3 lys2 leu2-k arg4-NspI hoΔLYS2*	Woltering *et al.* (2000)
AN120	<u>*MATα ura3 leu2 his3ΔSK trp1::hisG arg4-NspI lys2*</u>	Neiman *et al.* (2000)
	*MAT**a** ura3 leu2 his3ΔSK trp1::hisG ARG4 lys2*	
	<u>*hoΔ::LYS2 rme1Δ::LEU2*</u>	
	hoΔ::LYS2 RME1	
AN262	Same as AN120 except <u>*chs3Δ::HIS3MX6*</u>	Coluccio *et al.* (2004)
	chs3Δ::HIS3MX6	
AN264	Same as AN120 except <u>*dit1Δ::HIS3MX6*</u>	Coluccio *et al.* (2004)
	dit1Δ::HIS3MX6	
AN512	<u>*MAT**a** ura3 his3 leu2 trp1 LYS2 arg4 rme1Δ::LEU2*</u>	This study
	MATα ura3 his3 leu2 trp1 lys2 ARG4 RME1	
	<u>*srt1Δ::::kanMX6*</u>	
	srt1Δ::::kanMX6	
AN1092	*MATα ura3 his3ΔSK trp1::hisG arg4-NspI lys2 leu2 rme1Δ::LEU2 shc1Δ::HIS3MX6 hoΔ::LYS2*	This study
AN1093	*MAT**a** ura3 his3ΔSK trp1::hisG lys2 leu2 shc1Δ::HIS3MX6 hoΔ::LYS2*	This study
AN270	Same as AN120 except <u>*shc1Δ::HIS3MX6*</u>	This study
	shc1Δ::HIS3MX6	
CL50	Same as AN120 except <u>*cda1,2Δ:: hphMX3*</u>	Lin *et al.* (2013)
	cda1,2Δ:: hphMX3	
RHY1	*MAT**a** ura3 lys2 leu2 trp1-hisG his3ΔSK srt1Δ::kanMX6 ho::LYS2*	This study
RHY2	*MATα ura3 lys2 leu2-k arg4-NspI srt1Δ::kanMX6 hoΔLYS2*	This study
RHY19	<u>*MAT**a** ura3 lys2 leu2 trp1-hisG ARG4 his3ΔSK*</u>	This study
	MATα ura3 lys2 leu2-k TRP1 arg4-NspI HIS3	
	<u>*srt1Δ::kanMX6 hoΔ::LYS2*</u>	
	srt1Δ::kanMX6 hoΔ::LYS2	
RHY19-P1	Same as RHY19 with <u>pRS306-SRT1</u> (*URA3 SRT1*)	This study
	pRS306-SRT1	
RHY19-P2	Same as RHY19 with <u>pRS306-srt1-D75A</u> (*URA3 srt1-D75A*)	This study
	pRS306-srt1-D75A	
RHY27	*MATα ura3 leu2 his3ΔSK trp1Δ::hisG arg4-NspI lys2 rme1Δ::LEU2 chs4Δ::kanMX6 hoΔ::LYS2*	This study
RHY28	*MAT**a** ura3 leu2 his3ΔSK trp1Δ::hisG lys2 chs4Δ::kanMX6 hoΔ::LYS2*	This study
RHY29	Same as AN120 except <u>*chs4Δ::kanMX6*</u>	This study
	chs4Δ::kanMX6	
RHY23	Same as AN117-4B except *chs4Δ::kanMX6 shc1Δ::HIS3MX6*	This study
RHY24	Same as AN117-16D except *chs4Δ::kanMX6 shc1Δ::HIS3MX6*	This study
RHY26	Same as AN120 except <u>*chs4Δ::kanMX6 shc1Δ::HIS3MX6*</u>	This study
	chs4Δ::kanMX6 shc1Δ::HIS3MX6	
RHY37	*MATα ura3 leu2 his3ΔSK trp1Δ::hisG lys2 hoΔ::LYS2 chs4Δ::kanMX6 shc1Δ::HIS3MX6*	This study
RHY38	*MAT**a** ura3 leu2 rme1Δ::LEU2 his3ΔSK trp1Δ::hisG lys2 arg4-NspI hoΔ::LYS2 chs4Δ::kanMX6 shc1Δ::HIS3MX6*	This study
RHY39	Same As RHY26	This study
RHY16	Same as AN120, except <u>*CHS3::3xsfGFP::kanMX6*</u>	This study
	CHS3::3xsfGFP::kanMX6	
RHY42	Same as RHY16	This study
RHY44	Same as AN120 except <u>*CHS3-3xsfGFP::kanMX6 srt1Δ::kanMX6*</u>	This study
	CHS3-3xsfGFP::kanMX6 srt1Δ::kanMX6	

were used to inoculate 25 ml of Yeast Peptone Acetate (YPA) medium in 250 ml flasks to a final OD_{660} (optical density 660 nm) of 0.1–0.2 (usually a 1:25 or 2:25 dilution) and incubated overnight at 30° on a shaker at 250 rpm. Cell cultures with OD_{660} values between 0.7 and 1.3 were harvested in a Fischer Scientific Centrific centrifuge model 255 using a four-bucket model 215 rotor on setting 4 for 5 min. The cell pellets were washed once with water, pelleted in the same manner, and resuspended in SPO medium (2% KOAc) in 250 ml flasks to a final concentration of 2×10^7 cells/ml (a typical volume of 15–30 ml) and incubated with shaking at 30°. Spo20[51-91]-RFP was used to monitor progression through meiosis (Suda *et al.* 2007). For immunoblots and Chs3 activity assays, cells were harvested as soon as at least 60% of cells were post-meiotic as determined by prospore membrane morphology.

Fluorescence imaging

Imaging was performed using a Zeiss Observer.Z1 microscope with an attached Orca II ERG camera (Hamamatsu, Bridgewater, NJ). ZEN 2012 (Blue edition) software was used to acquire images. For imaging of lipid droplets, monodansylpentane (Abgent SM1000a) was used (Yang *et al.* 2012; Chen *et al.* 2017).

Table 2 Primers used in this study0

Name	Sequence
CK33	GTTCGGAGAAGGTTTAACAGTTCTGATTCTTTGCATTCTTTGAGTCGAAGCTTCAACTCGAGAGCGAAATCGGATCCCCGGGTTAATTAA
CK34	TAATTAAAAATGATGTAATATGGTAATAGGTATGGAAGAATCAGGGAGTTTTCAGAATGTTCTTTGCCCTGAATTCGAGCTCGTTTAAAC
RHO28	GTTAATAAGCCTTCCATTGTATACTACCAGGTTCTCGTCTTTTTTGGTGATAAAGTTAAAATAAAAGGATCGGATCCCCGGGTTAATTAA
RHO29	TTGTATCACTATATGCATTGAGTGTAAACTGTTGCACCTATAAAGAATGAAAACAATCTAGTATGTGTACGAATTCGAGCTCGTTTAAA
ANO274	AGTACGGTTGACATTACGAGTATCCCTTTGTTAAAATCAGGCAGTACCCATACGGATCCCCGGGTTAATTAA
ANO275	AGTTTAGTCTCCACAGTTTGTGAAAAAAAAAACAACAAAATAAAAGGAAAACGAAGTTTGTATTTATCTAGAATTCGAGCTCGTTTAAAC
YSO1	AAAGGGAAGATATTCTCAATCGGAAGGAGGAAAGTGACTCCTTCGTTGCACGGATCCCCGGGTTAATTAA
YSO2	ATAAGTTACACACAACCATATATCAACTTGTAAGTATCACAGTAAAAATAGAATTCGAGCTCGTTTAAAC
CK25	GTTCTTGCGGCCGCACTTCCGCTAACGCTGATGG
RHO07	GCCTCCCTCGAGAGGGGATTTCGATGACCTAG
RHO08	CTCCTTTATCATGGCTGGTAACCGGAGATA
RHO09	TATCTCCGGTTACCAGCCATGATAAAGGAG
RHO43	GCCTTCTTGACTTGGCATATCTCC
RHO44	GGGAACAAAAGCTGGGTACCACTTCCGCTAACGCTGATGG

Calcofluor White and Eosin Y staining

Staining was performed as described in Lin *et al.* (2013) with the following modifications. Prior to staining, 1 ml of cells were centrifuged at 5900 $\times$ *g* for 15 sec in a 2-ml microfuge tube, washed once with water, and resuspended in 250 μl water containing 1.0 mg/ml zymolyase (20,000 units/g; Amsbio). Cells were incubated at room temperature until spores were released from the asci, as determined by light microscopy, usually 5 min. Cells were centrifuged at 5900 $\times$ *g* for 15 sec, washed once in 1 ml McIlvaine's buffer [0.2 M Na$_2$HPO$_4$/0.1 M citric acid (pH 6.0)], and resuspended in 500 μl McIlvaine's buffer. Cells were stained by the addition of 30 μl Eosin Y disodium salt (Sigma) (5 mg/ml) for 10 min at room temperature in the dark. After staining, cells were washed three times in 500 μl of McIlvaine's buffer, until the supernatant was clear of residual Eosin Y, and then the cells were resuspended in 50–200 μl of McIlvaine's Buffer based on the size of the pellet; 7 μl of the final suspension was placed on a glass slide, to which 0.5 μl of 1 mg/ml Calcofluor White (CFW) was added prior to application of a cover slip. The spores were then visualized using filter cubes for blue (excitation 360 nm, emission 460 nm) or red (excitation 540 nm, emission 605 nm) fluorescence. All images were collected at the same exposure time; 560 msec for Eosin Y, 180 msec for CFW.

Electron microscopy

Cells viewed by transmission electron microscopy (TEM) were processed as described previously with minor modifications (Suda *et al.* 2007). Briefly, cells were collected in centrifuge tubes and fixed with 3% EM grade glutaraldehyde (Electron Microscopy Sciences) in 0.1 M sodium cacodylate (SC) buffer (pH 7.4) at room temperature. After fixation, samples were washed in SC buffer and resuspended in an aqueous 4% potassium permanganate solution, washed, stained with saturated uranyl acetate, dehydrated through a graded ethanol series (20–100%), and embedded in Epon resin (Electron Microscopy Sciences).

Alternately, after fixation, cells were rinsed in 0.1 M sodium phosphate buffer, pH 7.4, and resuspended in ultralow gelling temperature agarose (Promega) in 1.5 ml microfuge tubes. Agarose embedded samples were removed, and cut into smaller cubes with a scalpel. Samples were then suspended in aqueous 1% potassium permanganate, rinsed in 0.1 M phosphate buffer, treated with 0.5% sodium metaperiodate (Electron Microscopy Sciences), rinsed again, and dehydrated through a graded ethanol series. After dehydration, samples were embedded in Spurr's resin (Electron Microscopy Sciences) and polymerized in a 60° oven.

Ultrathin sections of 80 nm were cut with a Reichert-Jung UltracutE ultramicrotome and placed on formvar coated slot copper grids (Electron Microscopy Sciences). Sections were viewed with a FEI Tecnai12 BioTwinG^2 electron microscope located in the Stony Brook Center for Microscopy. Digital images were acquired with an AMT XR-60 CCD Digital Camera System.

Western blots

Lysis and protein preparation were performed as described in Knop *et al.* (1999) prior to loading on a 12% sodium dodecylsulfate-polyacrylamide gel with 1 mm spacers, prepared using a kit from Bio-Rad (#1610175). Samples were run for 20–30 min at 300 V. Blocking buffer was 6.5% (w/v) milk in TTBS (50 mM Tris, pH 7.5, 50 mM NaCl, 0.1% Tween 20). Primary anti-GFP antibodies (JL-8, Clontec) and anti-Por1 antibodies (Molecular Probes) were used at 1:1000 dilution in blocking buffer and applied for 1 hr with shaking at room temperature. Secondary sheep anti-mouse IgG antibodies coupled to horseradish peroxidase were diluted 1:2500 (GE Healthcare) and applied for 1 hr with shaking at room temperature. Enhanced Chemiluminescence reagent (Amersham) was used to develop the blots, and quantification was performed using ImageQuant software (GE Healthcare).

Chs3 activity assay

Chs3 activity assays were performed as in Lucero *et al.* (2002) with the following modifications. The wells of microtiter plates (Falcon #353219) were coated in wheat germ agglutinin (WGA) by the addition of 100 μl 50 μg/ml WGA in 2.5 mM Tris-HCl (pH 7.5) and incubation at room temperature

for >16 hr. WGA solution was removed by repeated washes involving immersion in distilled water followed by vigorous shaking to remove the water. Wells were blocked by the addition of 300 µl of blocking buffer [20 mg/ml bovine serum albumin (BSA) in 50 mM Tris–HCl, pH 7.5] followed by incubation at room temperature for 3 hr. The plates were stored at $-20°$ if not used immediately. Prior to use, plates were thawed at room temperature and the blocking buffer removed by shaking.

Sporulating cells were lysed by bead beating using a MP Biomedical FastPrep-24. Two pulses of 6 m/sec for 40 sec were used with a 3-min pause on ice between pulses. The beads were made of zirconia/silica and were 0.5 mm in diameter (BioSpec Products). Lysis buffer was 20 mM Tris-HCl, pH 8.0, containing 2 mM phenylmethylsulfonyl fluoride (PMSF), as well as protease and phosphatase inhibitor cocktails (Sigma). The total protein concentration of the lysates was determined using the Bio-Rad protein assay kit calibrated with BSA standards.

Fifty microliter of a $2\times$ reaction mixture consisting of 3.2 mM $CoCl_2$, 10 mM $NiCl_2$, 80 mM GlcNAc, and 4 mM UDP-GlcNAc in 100 mM Tris-HCl, pH 8, was added to each well. For each well run with reaction buffer, another well was run with a $2\times$ control mixture, which was identical except for lacking UDP-GlcNAc. Lysate and water were added to bring the total volume to 100 µl, and the final protein concentration to 0.33 µg/µl. Reactions were incubated for 90 min at 30°, and stopped by addition of 20 µl of 50 mM EDTA, which was mixed in by gentle shaking for 30 sec. The wells were then washed by repeated immersion of the plate in distilled water; 200 µl of 0.5 µg/ml wheat germ agglutinin bound to horseradish peroxidase (Sigma) in blocking buffer was then added to each well, and the plate was gently shaken and incubated for 15 min at room temperature. The plate was then washed by immersion in distilled water, and shaken to remove the water; 100 µl of 1-Step Ultra TMB-ELISA (3,3′,5,5′-tetramethylbenzidine; Pierce) was added to each well, and the plate immediately placed in a plate reader (Bio Tek Synergy 2, operated by Gen5 2.0), and a 0 min timepoint reading taken at OD_{600}. Further readings were taken at 2 min intervals and a 20 min endpoint. Results were analyzed as the average difference in activity between reaction and control samples. Statistical significance was assessed using one-way ANOVA and Tukey honest significant difference *post hoc* test.

Isolation of lipid droplets

Lipid droplet fractions were prepared as described in Athenstaedt (2010) with minor modifications. Briefly, vegetative cells or sporulating cells harvested by centrifugation were incubated for 10 min at 30° in 0.1 M Tris/SO_4 buffer, pH 9.4, 10 mM dithiothreitol. Then, cells were treated with zymolyase in 1.2 M sorbitol, 20 mM potassium phosphate buffer, pH 7.4, for 2 hr at 30°. Spheroplasts were pelleted, washed, and resuspended in 10 mM Tris HCl, pH 7.4, 12% (w/w) Ficoll 400, 0.2 mM EDTA, 1 mM PMSF homogenization buffer, to a final concentration of 0.5 g per cell wet weight

per milliliter, and homogenized with a Dounce homogenizer. The homogenate was centrifuged at 5000 $\times$ g for 5 min at 4°; the resulting supernatant was transferred into a centrifuge tube, overlaid with an equal volume of homogenization buffer, and centrifuged for 2 hr at 100,000 $\times$ g in an SW40 rotor (Beckman Coulter). After centrifugation, the floating layer was collected from the top of the gradient and resuspended in homogenization buffer. The suspension was transferred into a fresh tube, and overlaid with 10 mM Tris HCl, pH 7.4, 8% (w/w) Ficoll 400, 0.2 mM EDTA, and centrifuged for 1 hr at 100,000 $\times$ g. The floating layer was removed from the top of the gradient and suspended in 10 mM Tris-HCl, pH 7.4, 8% (w/w) Ficoll 400, 0.6 M sorbitol, 0.2 mM EDTA, and transferred to a fresh tube. The suspension was overlaid with 10 mM Tris-HCl, pH 7.4, 0.2 mM EDTA, 0.25 M sorbitol buffer. After a final centrifugation for 1 hr at 100,000 $\times$ g, a white layer of highly purified lipid droplets was collected from top of the gradient and saved for biochemical analysis.

The microsomal pellet from the initial 100,000 $\times$ g centrifugation was homogenized in 10 mM Tris-HCl, pH 7.4, 0.2 mM EDTA, 0.25 M sorbitol buffer, and the homogenate was then centrifuged at 100,000 $\times$ g. The final pellet was saved for enzymatic analysis of *cis*-prenyltransferase activity in the microsomal fraction. The protein concentration of the lipid droplet fraction was determined after removing the lipids by extraction with three volumes of diethyl ether.

Cis-Prenyltransferase measurements

Cis-Prenyltransferase activity was measured as previously described (Szkopińska *et al.* 1997) with minor modifications. In the assay, addition of radio-labeled isopentenyl pyrophosphate (IPP) groups to a farnesyl pyrophosphate (FPP) primer creates products that can be measured by the incorporation of radioactive label into a hydrophobic fraction. The reaction volume was 50 µl and contained 50 µM FPP), 100 µM [1-^{14}C]-IPP (55 mCi/mmol) (American Radiolabeled Chemicals), 25 mM Tris-HCl, pH 7.4, 1 mM $MgCl_2$, 20 mM 2-mercaptoethanol, 10 mM potassium fluoride, 10 µM zaragozic acid A, a membrane fraction containing 50 µg protein from the microsomal fraction, or 2 µg of protein from the purified lipid droplet fraction, and 50 µg of BSA. After 90 min incubation at 30°, the reaction was terminated by the addition of 1 ml of chloroform: methanol (3:2). The protein pellet was removed by centrifugation, and the supernatant was extracted three times with 1/5 volume of 10 mM EDTA, pH 8.0, in 0.9% NaCl solution. To analyze the products of the reaction, lipids before and after chemical dephosphorylation were loaded onto High Performance Thin Layer Chromatography Silica gel 60 Reverse Phase 18 (HPTLC Silica gel 60 RP-18) plates with a concentrating zone (Merck, Darmstadt, Germany), and run in acetone containing 50 mM H_3PO_4. Plates were exposed to a film and radiolabeled products were detected by autoradiography. To assess chain length of the polyprenols, internal standards of dolichol 19, and undecaprenol (American Radiolabeled Chemicals) were mixed with the sample after dephosphorylation and the unlabeled standards were visualized by exposure to iodine vapor.

To chemically dephosphorylate polyprenol pyrophosphate, the chloroform fraction was evaporated under nitrogen and lipids were incubated at 80° in 1 N HCl for 1 hr. Polyprenols were extracted three times with two volumes of hexane. The organic fraction was washed with 1/3 volume of water. To measure the incorporation of radioactive IPP into the isoprenoid fraction, a portion of the chloroform fraction was subjected to liquid scintillation counting using a Tri-Carb 2100TR Liquid Scintillation Analyzer (Packard) scintillation counter to detect the amount of ^{14}C in each sample.

Extraction of polyprenols and dolichols

To isolate polyprenols for analysis, either 300 mg of yeast cells or isolated lipid droplet fractions containing 19–50 μg of protein were suspended in 1 ml of 40% methanol. The suspension was subjected to saponification by incubation for 1 hr at 95° in the presence of 3 M KOH to hydrolyze fatty acid esters of dolichols and polyprenols. Lipids were further extracted from the samples by the modified Folch method (Szkopińska *et al.* 1997).

Analysis of dolichols and polyprenols by liquid chromatography-mass spectrometry (LC-MS)

Dolichols and polyprenols were analyzed by LC-MS (Guan and Eichler 2011). LC was performed using a Zorbax SB-C8 reversed-phase column (5 μm, 2.1 × 50 mm) (Agilent) at a flow rate of 200 μl/min with a linear gradient as follows: 100% of mobile phase A (methanol/acetonitrile/aqueous 1 mM ammonium acetate (60/20/20, v/v/v) was held isocratically for 2 min, and then linearly increased to 100% mobile phase B (100% ethanol containing 1 mM ammonium acetate) over 14 min, and held at 100% B for 4 min. A multiple reaction monitoring (MRM) protocol was performed in the negative ion mode using a 4000 Q-Trap hybrid triple quadrupole linear iontrap mass spectrometer equipped with a Turbo V ion source (AB-Sciex, Foster City, CA). The MS settings were as follows: curtain gas = 20 psi, ion source gas 1 = 20 psi, ion source gas 2 = 30 psi, ion spray = −4500 V, heater temperature = 350°, Interface Heater = ON, declustering potential = −40 V, entrance potential = −10 V, and collision exit potential = −5 V. The voltage used for collision-induced dissociation was −40 V. For the MRM pairs, the precursor ions are the [M+acetate]− adduct ions of dolichol and polyprenol species, and the product ions are the acetate ions (*m/z* 59).

Data availability

All the reagents and data described in this paper are freely available upon request to the corresponding author.

Results

SRT1 is required for outer spore wall formation

Previous work has demonstrated that *SRT1* is required to make zymolyase-resistant spores, suggesting it is involved
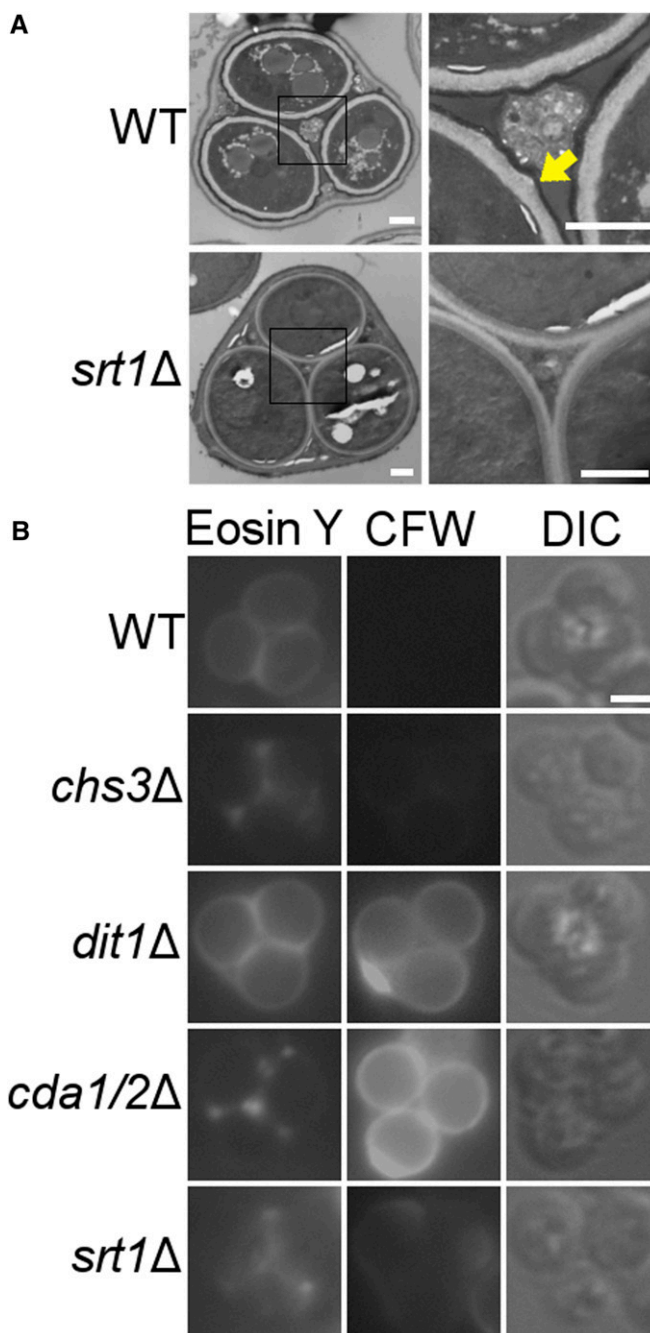

Figure 1 Cytological analysis of spore walls in *srt1*Δ and mutants defective in forming the chitosan layer. (A) Electron micrographs of wild-type (WT; AN120) and *srt1*Δ (RHY19) spores. Bar, 500 nm. Black squares in the left panels indicate areas shown in close-up in the right panels. The yellow arrow highlights the darkly staining chitosan and dityrosine layers. (B) Spores of wild type (AN120), *chs3*Δ (AN262), *dit1*Δ (AN264), *cda1*Δ *cda2*Δ (CL50), and *srt1*Δ (AN512) stained with Eosin Y or CFW. "DIC" indicates transmitted light images taken by differential interference contrast microscopy. Bar, 2 μm.

in either spore or spore wall formation (Deutschbauer *et al.* 2002; Enyenihi and Saunders 2003; Marston *et al.* 2004). The former possibility was ruled out by the observation that *srt1*Δ diploids formed asci at a frequency comparable to wild
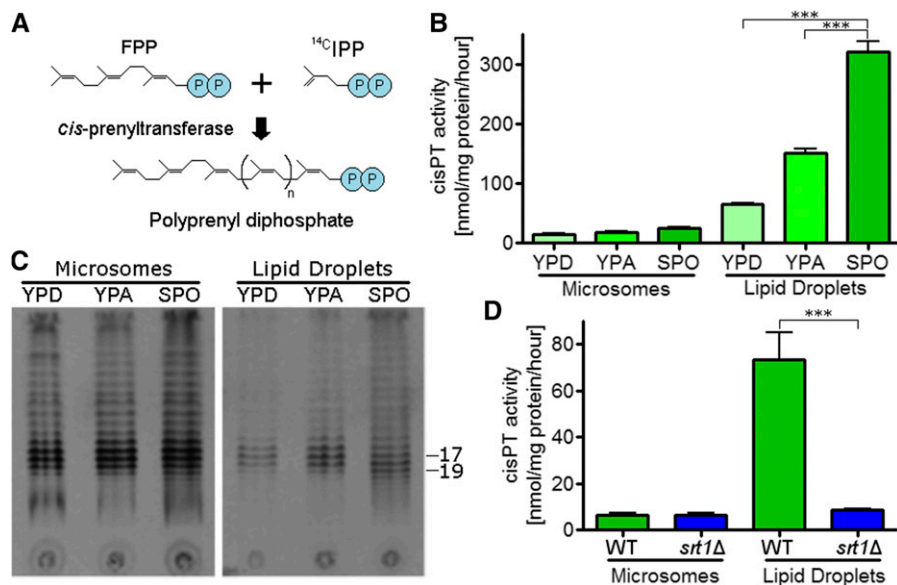
Figure 2 *Cis*-Prenyltransferase activity in glucose and acetate medium in vegetative and sporulating cells. (A) *In vitro* reaction catalyzed by *cis*-prenyltransferase. ^{14}C-labeled IPP units are serially attached to an FPP molecule to generate polyprenyl diphosphate containing variable numbers of IPP units (indicated by *n*). (B) Extracts were made from wild-type (RHY25) cells grown in YPD for 48 hr, grown in YPA until the OD_{600} reached ~ 2, or incubated in SPO medium for 7 hr. Extracts were separated into microsomal and lipid droplet fractions and assayed for *cis*-prenyltransferase activity. Asterisks (***) note significant differences between the samples indicated by brackets ($P < 0.001$) by one-way ANOVA followed by Tukey *post hoc* test. Error bars show SE. Activities shown are the averages of three experiments. (C) Autoradiogram of thin layer chromatography separation of the reaction products from (A). The position of species with 17 and 19 isoprene unit species are indicated. (D) *Cis*-Prenyltransferase activity from extracts of wild-type (AN120) and

srt1Δ (RHY19) cells incubated in SPO medium measured as in (A). Asterisks (***) note significant differences between the samples indicated by brackets ($P < 0.001$) by one-way ANOVA followed by Tukey *post hoc* test. Error bars show SE.

type (70.8% ±4.1 asci in wild type *vs.* 73.7% ±5.6 in *srt1Δ*). However, light microscopy does not have the resolution to detect spore wall defects, so TEM was used to compare the spore walls from wild-type and *srt1Δ* spores. As previously reported, wild-type spores contained both the lightly staining mannan and β-glucan inner spore wall layers, as well as the more darkly staining outer chitosan and dityrosine layers (Lynn and Magee 1970) (Figure 1A). In contrast, 100% of *srt1Δ* spores lacked the chitosan and dityrosine layers (Figure 1A). This phenotype closely resembles that observed for mutants deficient in the production or assembly of the chitosan layer, such as *chs3Δ* or *cda1Δ cda2Δ* (Pammer *et al.* 1992; Christodoulidou *et al.* 1999), suggesting that *SRT1* is required for chitosan synthesis.

The absence of the chitosan layer (and therefore also the dityrosine layer) can occur due either to a failure to synthesize chitin (*e.g.*, *chs3Δ*) or failure to assemble chitin into a chitosan layer, (*e.g.*, *cda1Δ cda2Δ*) (Pammer *et al.* 1992; Christodoulidou *et al.* 1996, 1999). These two possibilities can be differentiated using the stains CFW and Eosin Y (Lin *et al.* 2013). Eosin Y specifically stains chitosan, while CFW stains both chitosan and chitin, but has difficulty penetrating the dityrosine layer of a wild-type spore (Tachikawa *et al.* 2001; Baker *et al.* 2007). As such, wild-type spores stain in a solid ring around the spore by Eosin Y but poorly by CFW (Figure 1B). A mutant that does not produce the dityrosine layer, such as *dit1Δ*, stains in a solid ring with both dyes, while spores deficient in chitin production, such as *chs3Δ*, do not stain well with either dye (though Eosin Y staining can be seen in patches in the ascal cytoplasm between the spores) (Figure 1B). Spores that produce chitin but fail to convert it to chitosan, such as *cda1Δ cda2Δ*, stain brightly in rings with CFW, but Eosin Y is restricted to the ascal cytoplasm (Figure 1B). In these assays, *srt1Δ* spores phenocopy *chs3Δ* (Figure 1B). That is, they are not clearly stained by

CFW, and Eosin Y shows only patchy staining in the ascus, suggesting that the *srt1Δ* mutant lacks the outer spore wall layers due to a defect in chitin synthesis.

Sporulating cells display an SRT1-dependent increase in cis-prenyltransferase activity and long-chain polyisoprenoids

The outer spore wall defect of *srt1Δ*, along with a lack of phenotype for the deletion in vegetative cells, suggests that the Srt1-Nus1 *cis*-prenyltransferase functions primarily during sporulation. *cis*-Prenyltransferase activity can be monitored *in vitro* using an enzyme assay in which the enzyme serially attaches ^{14}C labeled IPP units to FPP (Figure 2A) (Grabińska *et al.* 2016). *cis*-Prenyltransferase activity was compared between microsomal and lipid droplet fractions derived from either vegetative cells grown in rich medium containing either glucose or acetate as the carbon source (YPD and YPA, respectively) or sporulating cells. *Cis*-Prenyltransferase activity was low in the microsomal fractions under all three conditions (Figure 2B). In contrast, activity was significantly increased in the lipid droplet fraction when cells were grown in acetate compared to glucose, and activity was further increased by incubation in SPO medium (which is 2% KOAc) (Figure 2B). The reaction products were visualized using thin-layer chromatography and autoradiography, which revealed that the most prominent species in both the microsome and lipid droplet fractions from vegetative cells were centered on 16–17 isoprene units, consistent with Rer2 being the predominant synthase (Sato *et al.* 2001) (Figure 2C). By contrast, a shift toward longer species ($\sim$19 units) was observed specifically in the lipid droplet fraction from sporulating cells. The fact that Srt1-Nus1 generates longer polyprenoids than Rer2-Nus1, and that Srt1 localizes to lipid droplets in sporulating cells (Sato *et al.* 2001; Schenk *et al.*
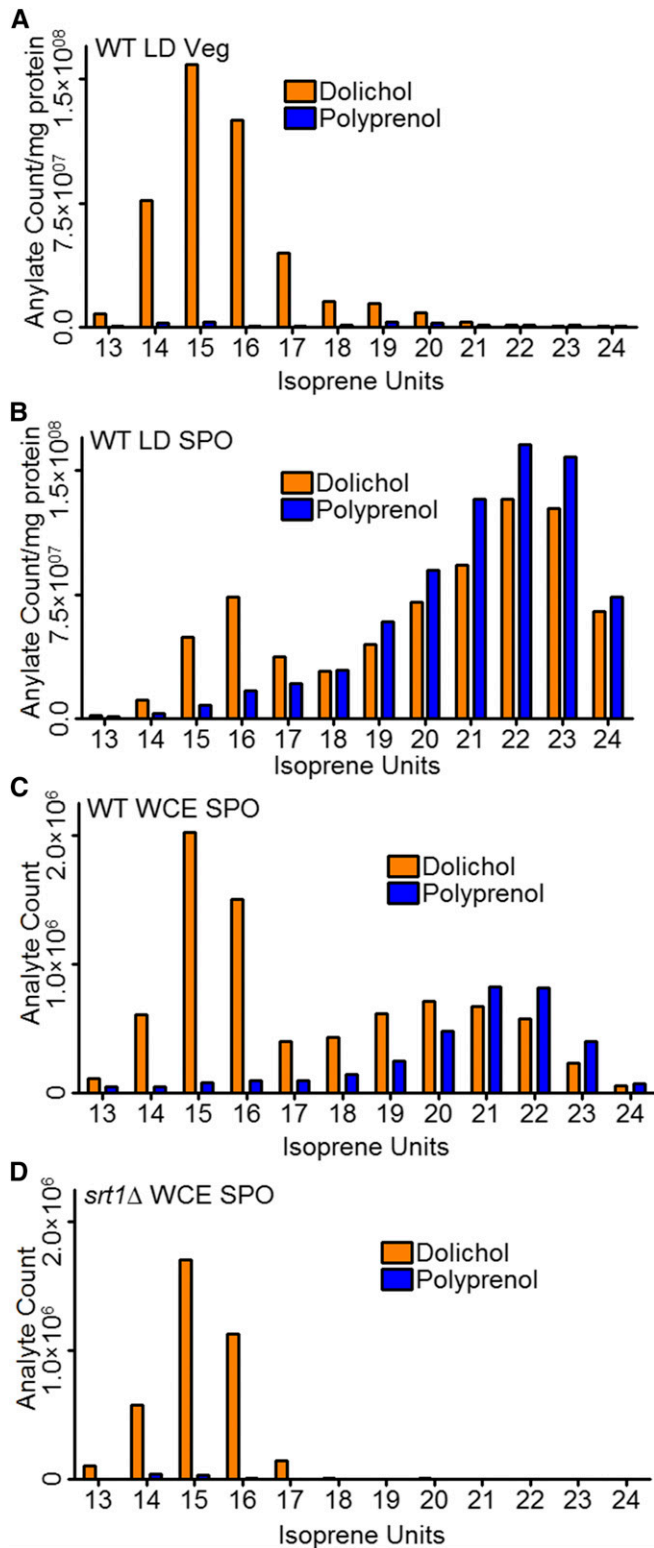
Figure 3 Various dolichol and polyprenol species isolated from lipid droplets in vegetative and sporulating cells. (A) The distribution of dolichol and polyprenol molecules containing different numbers of isoprene units was determined by LC-MS analysis of lipid droplet (LD) fractions from wild-type (WT) (AN120) cells grown in YPD for 48 hr (Veg), normalized against the total protein present in the fraction. (B) As in (A), except using sporulating cells incubated in SPO medium for 7 hr. (C) As in (A),

2001; Lam *et al.* 2014), suggested that the sporulation-specific *cis*-prenyltransferase activity observed in lipid droplets is due to *SRT1*. This idea was confirmed by the observation that the sporulation-specific increase in *cis*-prenyltransferase activity observed in the lipid droplets was eliminated in *srt1Δ* (Figure 2D).

Given that Srt1-Nus1 is the predominant *cis*-prenyltransferase activity in sporulating cells, the levels of long-chain polyisoprenoids should be increased in sporulating cells compared to vegetative cells. This is indeed the case. The distribution of both dolichol and polyprenols containing different numbers of isoprene units present in lipid droplets from either vegetative or sporulating cells was determined using LC-MS. In lipid droplets from vegetative cells, the predominant isoprenoids were dolichols of 14–17 repeats (Figure 3A). By contrast, in sporulating cells the predominant species were longer (21–23 repeats) (Figure 3B). Moreover, the longer polyprenols were not efficiently converted to dolichol, as has been reported previously for Srt1 products (Sato *et al.* 2001). To determine whether the increased amounts of long-chain isoprenoids seen in sporulating cells are *SRT1*-dependent, whole cell lysates of sporulating cultures of wild-type and *srt1Δ* cells were assayed by LC-MS. While 14–17 unit dolichols were present in both cultures, the long-chain polyprenols and dolichols were absent in *srt1Δ* cells (Figure 3, C and D). Together, these results demonstrate an *SRT1*-mediated increase of long-chain polyisoprenoids in lipid droplets during sporulation, which may be linked with the requirement for *SRT1* in outer spore wall formation.

The cis-prenyltransferase activity of Srt1 is necessary for outer spore wall formation

SRT1-dependent polyprenols increase during sporulation and *SRT1* is required for making the chitosan layer of the outer spore wall, raising the possibility that polyprenols are necessary for formation of the chitosan layer. This hypothesis was tested by phenotypically characterizing diploids containing an allele of *SRT1* that encodes a catalytically inactive version of the enzyme. Aspartate (D) at position 27 of the *E. coli cis*-prenyltransferase undecaprenyl pyrophosphate synthase (UPPS) is required for catalysis (Pan *et al.* 2000). Alignment of the UPPS and Srt1 protein sequences identified D75 of Srt1 as the cognate residue for UPPS D27 (Figure 4A). (Liang *et al.* 2002). Measurements of *cis*-prenyltransferase activity in lipid droplets from sporulating cells for *SRT1*, *srt1Δ*, and *srt1-D75A* diploids showed that *srt1Δ* and *srt1-D75A* both lack this activity, indicating that the D75A mutation creates a null phenotype with regard to enzyme activity (Figure 4B). Immunoblot analysis of GFP-tagged versions of Srt1 and Srt1-D75A demonstrated that the reduction in activity observed for *srt1-D75A* is not due to protein instability (Figure 4C). In sporulating cells, Srt1 is localized to lipid

except using whole cell extracts (WCE) of WT (AN120) cells incubated in SPO medium for 7 hr. (D) As in (D), except using WCE of *srt1Δ* cells (RHY19).
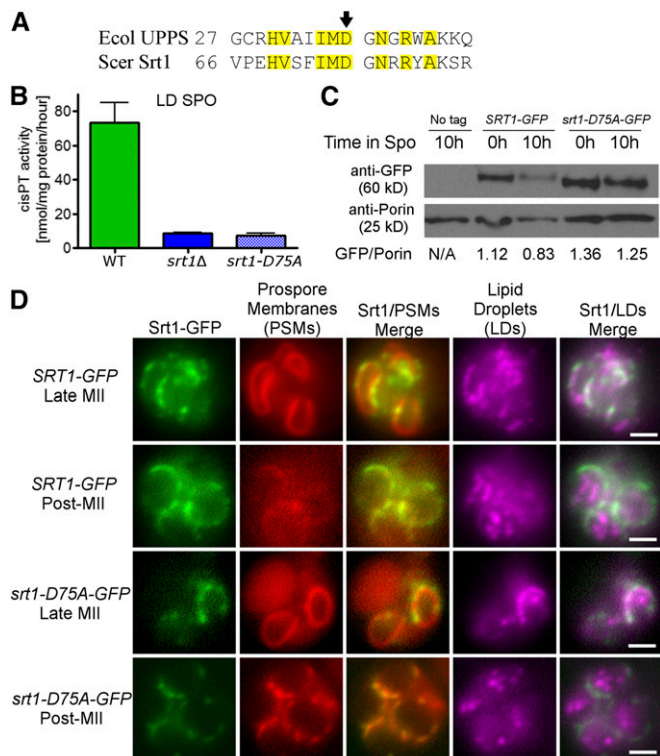
Figure 4 A catalytic site mutant of Srt1. (A) Alignment of *E. coli* (Ecol) undecaprenyl pyrophosphate synthase (UPPS) and *S. cerevisiae* (Scer) Srt1 protein sequences. Numbers indicate the amino acid position in the protein of the first amino acid shown in the sequence. Identical residues are highlighted in yellow; the black arrow indicates the aspartate residue mutated in *srt1-D75A*. (B) LD fractions were prepared from sporulating cells of wild type (AN120), *srt1Δ* (RHY19), or *srt1-D75A* (RHY19-P2) and assayed for *cis*-prenyltransferase activity. (C) Lysates of wild-type (AN120) cells carrying no plasmid, or plasmids expressing *SRT1-GFP* or *srt1-D75A-GFP* were prepared at the time of transfer (0 hr) or 10 hr after transfer to SPO medium. Western blots were performed using anti-GFP antibodies or anti-Porin antibodies as a loading control. The ratio of Srt1:Por1 signal is shown below. (D) Sporulating wild-type (AN120) cells expressing *SRT1-GFP* or *srt1-D75A-GFP* (green) and the prospore membrane marker Spo20$^{51-91}$-RFP (red), were stained with the LD marker monodansylpentane (violet) and examined by fluorescence microscopy. Representative cells from different stages are shown. Bar, 2 μm.

droplets associated with prospore membranes (Lam *et al.* 2014). To compare the localization of the wild-type and mutant proteins, the prospore membrane marker Spo20$^{51-91}$-RFP (Suda *et al.* 2007) was introduced into diploids carrying either *SRT1-GFP* or *srt1-D75A-GFP*. In addition, sporulating cells were stained with the hydrophobic blue fluorescent marker, monodansylpentane, to visualize lipid droplets (Yang *et al.* 2012; Currie *et al.* 2014), and all three markers were detected by fluorescence microscopy. As previously described, Srt1-GFP was found in puncta along the extending prospore membrane (Lam *et al.* 2014), and these puncta also stained with the lipid droplet marker (Figure 4D). In post-MII cells (indicated by large, round, prospore membranes), Srt1-GFP fluorescence was seen in patches around the outside of the spore. These patches no longer colocalized with the lipid droplet dye, consistent with the
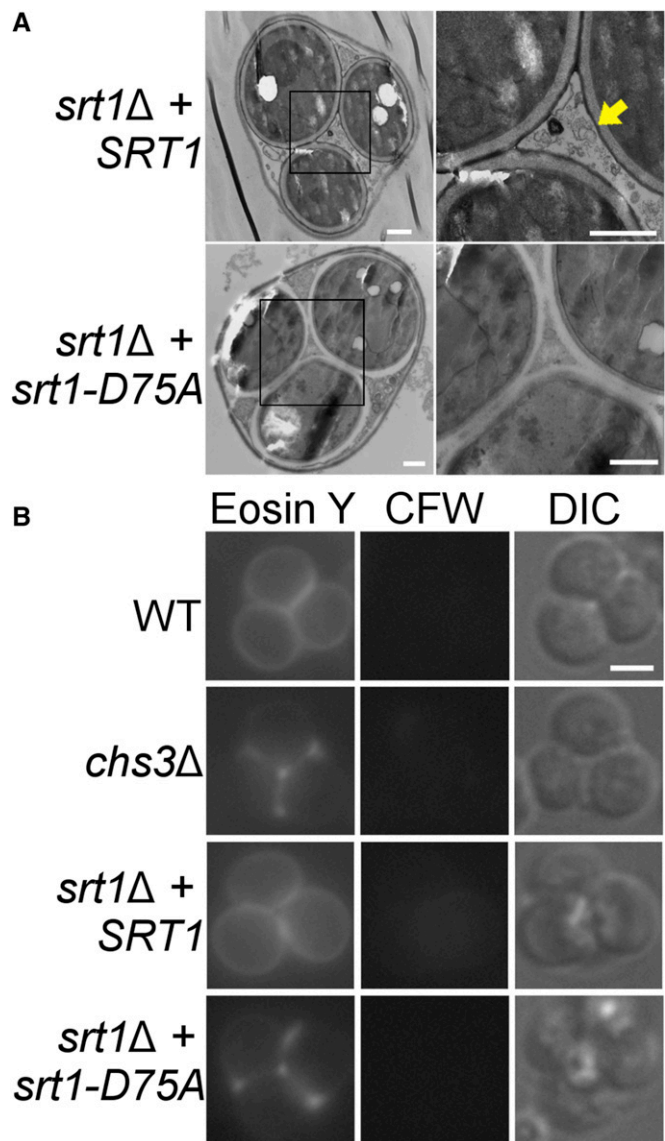

Figure 5 Analysis of spore walls of *srt1-D75A* spores. (A) Electron micrographs of *srt1Δ* cells transformed with integrating plasmids carrying *SRT1* (RHY19-P1; top panels) or *srt1-D75A* (RHY19-P2; bottom panels). Yellow arrow indicates the dark staining outer spore wall, areas are in close-up are indicated by black boxes. Bar, 500 nm. (B) Spores of WT (AN120), *chs3Δ* (AN264), *srt1Δ* expressing *SRT1* (RHY 19-P1), or *srt1Δ* expressing *srt1-D75A* (RHY19-P2), were stained with Eosin Y and CFW. "DIC" indicates transmitted light images taken by differential interference contrast microscopy. Bar, 2 μm.

disappearance of lipid droplets outside of the prospore membrane after closure (Figure 4D) (Ren *et al.* 2014). The same patterns were observed for Srt1^{D75A}-GFP; thus, the mutant protein is inactive but stable and properly localized. The *srt1-D75A* mutant is therefore a useful tool to examine which phenotypes of *SRT1* are dependent on its enzymatic activity.

SRT1-dependent *cis*-prenyltransferase activity is required for generation of the chitosan layer in spores. TEM analysis of *srt1-D57A* spores revealed that the darkly staining material indicative of the chitosan and dityrosine layers of the spore
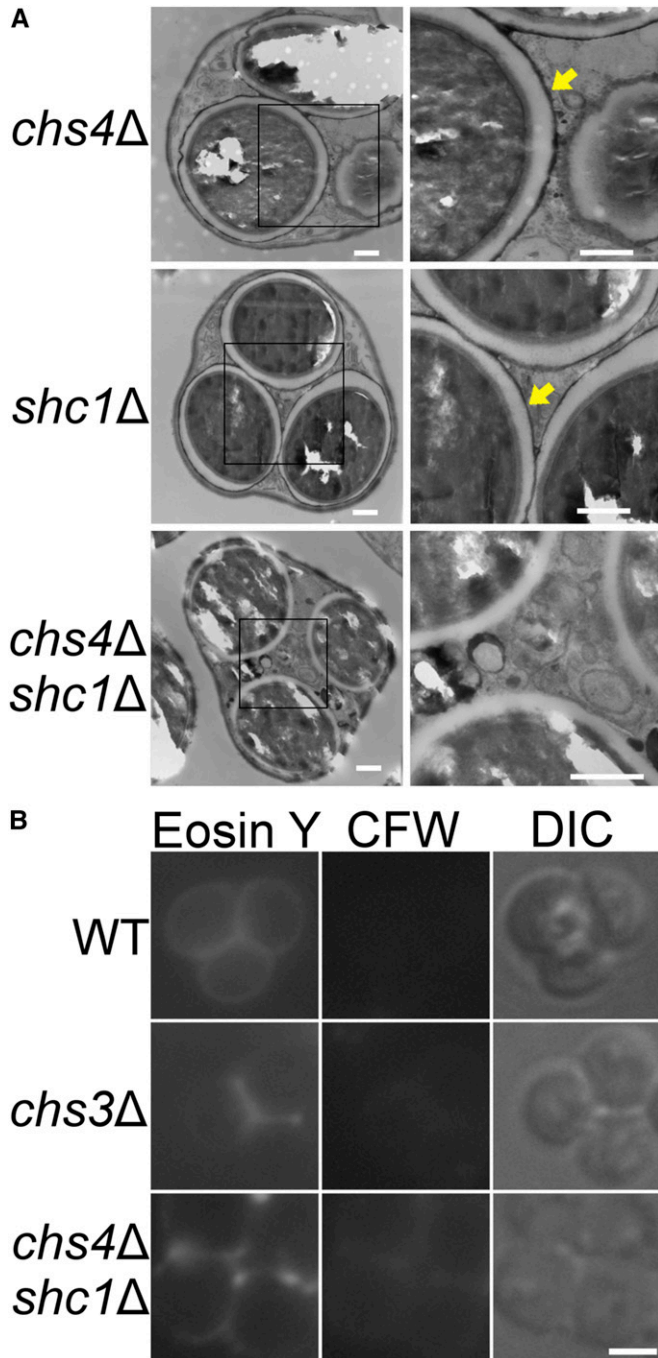
A

B

Figure 6 Analysis of spore walls in *chs4Δ*, *shc1Δ*, and *chs4Δ shc1Δ* cells. (A) Electron micrographs of *chs4Δ* (RHY29), *shc1Δ* (AN270), or *chs4Δ shc1Δ* (RHY39) spores. Bar, 500 nm. Black squares in left panels indicate areas in close-up view in the right panels. The yellow arrows highlight the darkly staining chitosan and dityrosine layers. (B) Spores of wild type or *chs4Δ shc1Δ* stained with Eosin Y or CFW. "DIC" indicates transmitted light images taken by differential interference contrast microscopy. Bar, 2 μm.

wall was absent, similar to *srt1Δ* (compare Figure 1A and Figure 5A). The absence of both chitin and chitosan was shown by the failure to observe any staining with either CFW or Eosin Y (Figure 5B). These observations demonstrate
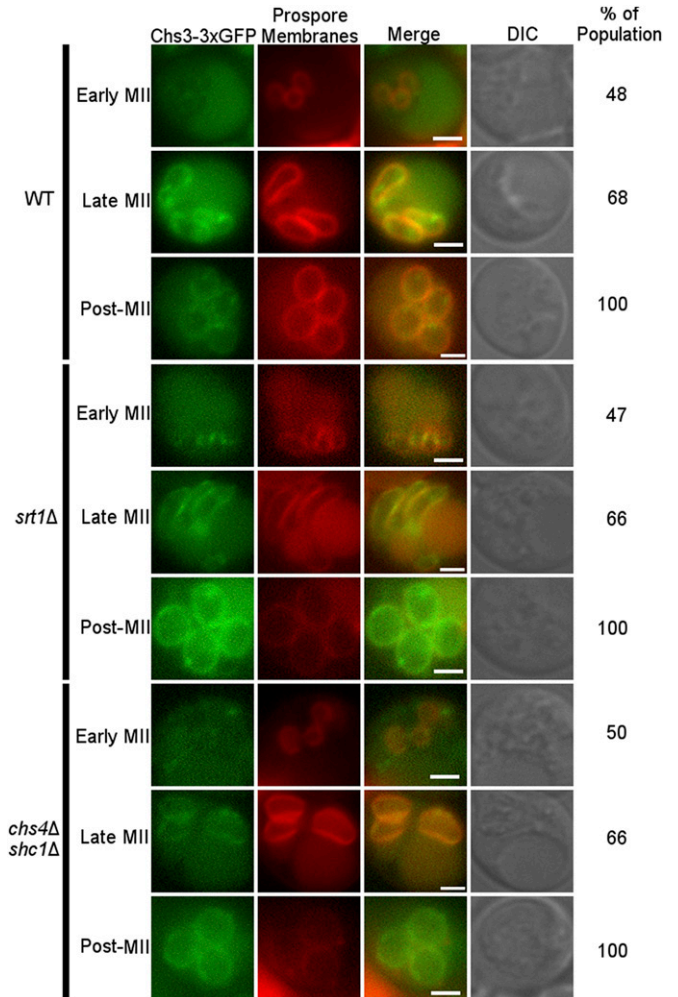

Figure 7 Chs3 localization in sporulating cells. Sporulating wild-type (RHY16), *srt1Δ* (RHY44), and *chs4Δ shc1Δ* (RHY57) cells expressing Chs3-3xGFP (green) and the prospore membrane marker Spo20[51-91]-RFP (red) were examined by fluorescence microscopy. Representative cells in early MII, late MII, and postmeiosis are shown. Numbers at right indicate the percentage of cells at each stage with displaying Chs3-GFP localization at the prospore membrane. Bar, 2 μm.

that Srt1-generated polyprenols are required specifically for the formation of the chitosan layer of the outer spore wall.

CHS4 and SHC1 act redundantly to promote outer spore wall formation

Synthesis of the chitosan layer of the spore wall requires first that chitin be generated by the chitin synthase, Chs3 (Pammer *et al.* 1992). In vegetative cells, Chs3 activity is controlled by the allosteric activator, Chs4 (DeMarini *et al.* 1997; Ono *et al.* 2000; Kozubowski *et al.* 2003). In sporulating cells, there is a sporulation-specific paralog of Chs4 called Shc1 (Sanz *et al.* 2002). *CHS4* and *SHC1* function redundantly during sporulation to make the chitosan layer of the spore wall—*i.e.*, spore walls were normal in either single mutant while both the chitosan and dityrosine layers were absent in the *chs4Δ shc1Δ* double mutant (Figure 6A). These cytological phenotypes
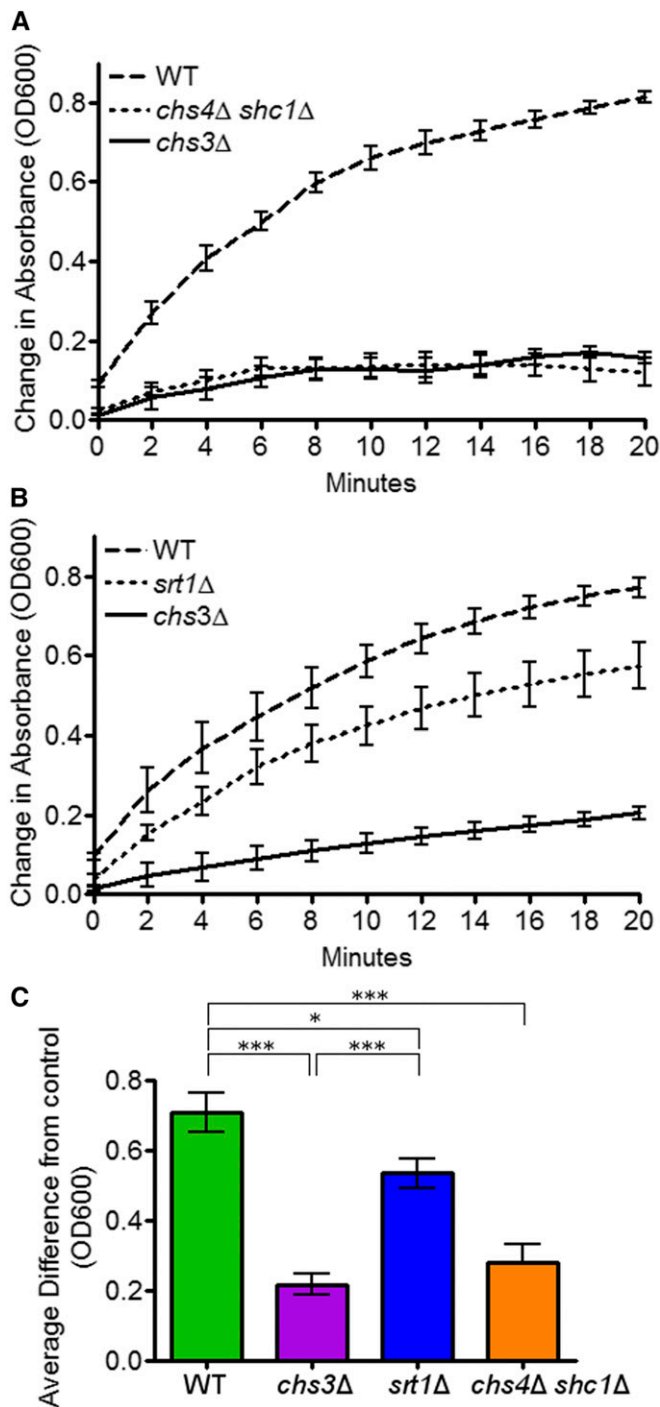
Figure 8 Chs3 activity in various mutants in sporulating cells. Chitin synthase activity assays were performed as a function of time after addition of the horseradish peroxidase substrate using extracts from sporulating cultures as described in *Materials and Methods*. Assays were performed in quadruplicate at 2-min intervals over a 20-min time-course six independent times. Representative time courses are shown. (A) Wild-type (AN210), *chs3Δ* (A262), and *chs4Δ shc1Δ* (RHY26). (B) Wild type, *chs3Δ* and *srt1Δ* (RHY19). (C) End point measurements of Chs3 activity (20-min time point) averaged across at least three experiments run in quadruplicate using the same strains as in (A) and (B). Error bars show SE. Asterisks indicate significant difference (*$P < 0.05$; ***$P < 0.001$) assessed by one-way ANOVA followed by Tukey HSD *post hoc* test.

were confirmed by CFW and Eosin Y staining in which the *chs4Δ shc1Δ* spores resemble *chs3Δ* (Figure 6B). The discovery that eliminating known regulators of Chs3 activity (*chs4Δ shc1Δ*) has the same outer spore wall defect as *srt1-D57A* suggests a role for polyprenols in the regulation of chitin synthase activity specifically in sporulating cells.

SRT1 is not required for Chs3 localization to the prospore membrane

In vegetative cells, Chs3 activity is controlled, in part, by the regulated delivery of the protein to its site of action at the bud neck (Kozubowski *et al.* 2003). One mechanism by which Srt1 could facilitate Chs3 activity would be to promote the localization of Chs3 to the prospore membrane. This idea was tested by tagging Chs3 with 3xsfGFP in the genome of wild type, *srt1Δ*, and *chs4Δ shc1Δ* cells that contained Spo20[51-91]-RFP as a prospore membrane marker, and examining cells either at early, late, or post-MII for the colocalization of these markers.

Prospore membranes form and expand through a series of stages identifiable by the size and shape of the membrane (Diamond *et al.* 2009). At early MII in wild-type cells, about half of the prospore membranes displayed Chs3-3xsfGFP fluorescence (Figure 7). As the prospore membranes expanded through meiosis, the fraction that displayed Chs3-3xsfGFP fluorescence increased so that post-MII, and prior to chitin synthesis, 100% of the membranes contained detectable levels of Chs3 (Figure 7) (Coluccio *et al.* 2004). These results argue against the idea that Chs3 activity is controlled primarily by regulation of its localization to prospore membranes during sporulation. In fact, the pattern and timing of delivery of Chs3-3xsfGFP to the prospore membrane was very similar in the wild-type, *chs4Δ shc1Δ*, and *srt1Δ* diploids (Figure 7), suggesting that Srt1 may regulate instead the enzymatic activity of Chs3.

SRT1 promotes Chs3 activity in vitro

To test whether Srt1 regulates Chs3 activity *in vitro*, chitin synthase activity was measured in extracts from in *srt1Δ*, *chs4Δ shc1Δ*, *chs3Δ*, and wild-type sporulating cells (Lucero *et al.* 2002). Each strain was incubated in SPO medium until at least 60% of cells in the culture displayed refractile spores, indicating a majority of cells had completed formation of the β-glucan layer of the spore wall (Coluccio *et al.* 2004). Extracts were made from each culture, and equivalent amounts of protein added to reaction buffer containing the Chs3 substrate UDP-GlcNAc in 96-well plates coated with a chitin-binding lectin. The reactions were incubated at 30° for 90 min to allow Chs3 to covalently join the GlcNAc sugars to form chitin. This chitin binds to the lectin coating the wells. The wells were then rinsed to remove Chs3 and unreacted UDP-GlcNAc and the treated with a lectin-coupled horseradish peroxidase that binds to the chitin to form a "lectin sandwich." The amount of peroxidase bound is proportional to the amount of chitin synthesized (Lucero *et al.* 2002). The colorimetric horseradish peroxidase substrate, 3,3′,5,5′-tetramethylbenzidine,
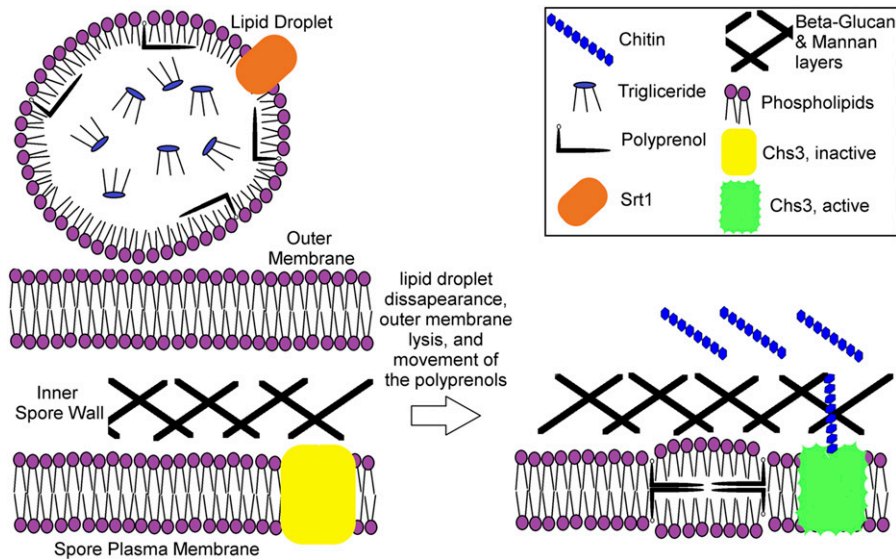
Figure 9 Model for the role of polyprenols in activation of Chs3. During the early stages of spore wall assembly, LDs associated with the outer membrane accumulate high levels of polyprenols (left panel). As the inner spore wall layers form, the neutral lipids in these droplets are consumed and the outer membrane lyses leading to the partition of the polyprenols into the spore plasma membrane (right panel). The presence of polyprenols in the spore plasma membrane serves a signal, directly or indirectly, to activate Chs3.

was then added to each well and the amount of peroxidase activity was measured using a spectrophotometer to measure the OD_{600} (Lucero *et al.* 2002). To control for the presence of chitin in the extracts or other forms of background, each extract was also incubated in wells lacking UDP-GlcNAc. The amount of chitin synthase activity was defined as the difference between the peroxidase activity in the wells with UDP-GlcNAc minus the peroxidase activity in the wells without UDP-GlcNAc.

Chitin synthase activity in the different strains was compared both as a function of time after addition of 3,3′,5,5′-tetramethylbenzidine (Figure 8, A and B), as well as at a 20 min endpoint (Figure 8C). Wild-type and *chs3Δ* extracts displayed a clear, statistically significant difference in chitin synthase activity (Figure 8) (Lucero *et al.* 2002). A significant reduction of activity was also seen in *chs4Δ shc1Δ* extracts, consistent with the known roles of these proteins as activators of Chs3 (Figure 8, A and C) (Ono *et al.* 2000; Sanz *et al.* 2002). The *srt1Δ* diploid exhibited a modest, but significant, decrease in activity compared to wild type (Figure 8, B and C). Although the decrease in chitin synthase activity is not as great as *chs4Δ shc1Δ*, the fact that *srt1Δ* and *chs4Δ shc1Δ* both fail to make outer spore walls suggests that *SRT1* is required to generate a threshold level of chitin synthase activity necessary for making the chitosan layer of the outer spore wall.

Discussion

In many systems, dynamic lipid droplets have emerged as a means to deliver lipids to specific locations in the cell (Kohlwein *et al.* 2013; Wang 2015). While cells that fail to produce triglycerides or sterol esters—the major components of lipid droplets—still form spores, cells that do not form lipid droplets at all show severe sporulation defects, often producing dead spores or no spores (Hsu *et al.* 2017). This suggests that, during sporulation, lipid droplets act as carriers for

additional proteins or lipids whose delivery to the prospore membrane or spore wall is important for spore formation. In the case of spore wall assembly, the lipid droplets are likely acting as carriers of polyisoprenoids. In addition to Srt1, the Lds family proteins localize specifically to external lipid droplets during sporulation (Lin *et al.* 2013). Loss of these proteins also causes outer spore wall defects, though the defect is distinct from *srt1Δ* in that the chitosan layer is present (Lin *et al.* 2013). Thus, the lipid droplets may deliver additional factors that are important for outer spore wall assembly.

The lipid droplets on which Srt1 is localized disappear over the course of spore wall maturation, presumably because the neutral lipids are consumed, as evidenced by their reduction in size seen in TEM, the disappearance of staining with hydrophobic dyes, and the change in localization of proteins like Srt1 from these droplets to a distribution around the spore (Lin *et al.* 2013; Ren *et al.* 2014). As these droplets disappear, the polyisoprenoids in them must partition into a different hydrophobic environment. As synthesis of the β-glucan layer finishes, the outer membrane lyses (Coluccio *et al.* 2004) (Figure 9). Thus, the nearest cellular membrane to which the polyisoprenoids "released" from the lipid droplets could move to is the spore plasma membrane. We propose that the appearance of these long chain polyisoprenoids in the spore plasma membrane directly or indirectly activates the chitin synthase, Chs3, to make the chitin necessary for formation of the chitosan layer, thereby coordinating outer spore wall assembly with the completion of the inner spore wall (Figure 9).

There are several possible ways that delivery of polyisoprenoids to the spore plasma membrane might promote chitin synthesis. Given the well-characterized role of dolichols as sugar carriers for protein glycosylation (Burda and Aebi 1999; Loibl and Strahl 2013), one possibility is that *SRT1*-generated polyprenols play a similar role as sugar carriers for spore wall assembly. The explanation is unlikely, however, given that the mannan layer (which is composed of N- and O-mannosylated

proteins) is properly formed in the *srt1Δ* mutant, indicating there is no major deficit in protein glycosylation. Also, the sugar donor for chitin synthesis is the cytoplasmic sugar nucleotide UDP-GlcNAc (Cabib *et al.* 1983; Pammer *et al.* 1992), so there is no need for dolichol to act as a sugar carrier in this reaction. It is noteworthy that in brine shrimp, it has been suggested that the synthesis of chitin may be primed by an initial GlcNAc residue linked to dolichol (Horst 1983). While no such requirement has been reported for yeast chitin synthases, it is possible that the long-chain polyprenols produced by Srt1 could be conjugated to GlcNAc and act as primers for Chs3 to begin synthesis at the spore plasma membrane. Dolichol not only acts as a carrier for the sugars in N-linked glycosylation, but the lipid is important for allowing the dolichol-linked sugars to flip from the cytosolic to luminal side of the ER membrane (Sanyal and Menon 2010; Perez *et al.* 2015). The transmembrane domains of the chitin synthase enzyme itself are proposed to form a pore to allow for translocation of the chitin chains across the plasma membrane, and there is structural data from related bacterial cellulose synthases to support this model (Cabib *et al.* 1983; Morgan *et al.* 2013; Gohlke *et al.* 2017). However, it is possible that polyprenols could facilitate translocation of the chains through their effects on properties of the membrane.

Alternatively, the presence of polyisoprenoids in the spore plasma membrane might directly activate Chs3. Polyprenols can affect the shape and fluidity of membrane bilayers in *in vitro* experiments (Valtersson *et al.* 1985). Recently it was reported that polyprenols influence photosynthetic performance *in vivo* through their modulation of thylakoid membrane dynamics in the chloroplast (Akhtar *et al.* 2017). For instance, Chs3 oligomerization is important for its chitin synthase activity (Gohlke *et al.* 2017), and this could be affected by the properties of the membrane. Finally, the effect on Chs3 activity might be indirect. Polyisoprenoids in the prospore membrane could act in a signaling pathway that regulates Chs3 activity. Mutations in two other genes, *MUM3* and *OSW1*, display similar phenotypes as *srt1Δ* (Coluccio *et al.* 2004), raising the possibility that they may act with *SRT1* in such a pathway.

While the precise mechanism by which polyisoprenoids lead to activation of Chs3 remains to be determined, our results reveal a function for these lipids separate from their known role in protein glycosylation. Dolichol and other polyprenols are present in all kingdoms of life and, in eukaryotic cells, are found in membrane compartments outside of the ER where glycosylation occurs (Swiezewska and Danikiewicz 2005; Jones *et al.* 2009). Any mechanism by which Srt1-generated polyprenols promote spore wall formation may therefore be conserved in other fungi for activation of chitin synthase or, potentially, in other organisms for other, unrelated, processes.

Literature Cited

Abu-Qarn, M., J. Eichler, and N. Sharon, 2008 Not just for Eukarya anymore: protein glycosylation in Bacteria and Archaea. Curr. Opin. Struct. Biol. 18: 544–550.

Akhtar, T. A., P. Surowiecki, H. Siekierska, M. Kania, K. Van Gelder *et al.*, 2017 Polyprenols are synthesized by a plastidial *cis*-prenyltransferase and influence photosynthetic performance. Plant Cell 29: 1709–1725.

Athenstaedt, K., 2010 Isolation and characterization of lipid particles from yeast, pp. 4223–4229 in *Handbook of Hydrocarbon and Lipid Microbiology*, edited by K. N. Timmis. Springer, Berlin.

Bahler, J., J. Q. Wu, M. S. Longtine, N. G. Shah, A. McKenzie, III *et al.*, 1998 Heterologous modules for efficient and versatile PCR-based gene targeting in *Schizosaccharomyces pombe*. Yeast 14: 943–951.

Baker, L. G., C. A. Specht, M. J. Donlin, and J. K. Lodge, 2007 Chitosan, the deacetylated form of chitin, is necessary for cell wall integrity in *Cryptococcus neoformans*. Eukaryot. Cell 6: 855–867.

Briza, P., A. Ellinger, G. Winkler, and M. Breitenbach, 1988 Chemical composition of the yeast ascospore wall. The second outer layer consists of chitosan. J. Biol. Chem. 263: 11569–11574.

Briza, P., M. Breitenbach, A. Ellinger, and J. Segall, 1990a Isolation of two developmentally regulated genes involved in spore wall maturation in *Saccharomyces cerevisiae*. Genes Dev. 4: 1775–1789.

Briza, P., A. Ellinger, G. Winkler, and M. Breitenbach, 1990b Characterization of a DL-dityrosine-containing macromolecule from yeast ascospore walls. J. Biol. Chem. 265: 15118–15123.

Burda, P., and M. Aebi, 1999 The dolichol pathway of N-linked glycosylation. Biochim. Biophys. Acta 1426: 239–257.

Byers, B., 1981 Cytology of the yeast life cycle, pp. 59–96 in *The Molecular Biology of the Yeast Saccharomyces: Life Cycle and Inheritance*, edited by J. N. Strathern, E. W. Jones, and J. R. Broach. Cold Spring Harbor Laboratory Press, Cold Spring Harbor, NY.

Cabib, E., B. Bowers, and R. L. Roberts, 1983 Vectorial synthesis of a polysaccharide by isolated plasma membranes. Proc. Natl. Acad. Sci. USA 80: 3318–3321.

Chen, B. H., H. J. Yang, H. Y. Chou, G. C. Chen, and W. Y. Yang, 2017 Staining of lipid droplets with monodansylpentane. Methods Mol. Biol. 1560: 231–236.

Choi, W. J., A. Sburlati, and E. Cabib, 1994 Chitin synthase 3 from yeast has zymogenic properties that depend on both the *CAL1* and the *CAL3* genes. Proc. Natl. Acad. Sci. USA 91: 4727–4730.

Christodoulidou, A., V. Bouriotis, and G. Thireos, 1996 Two sporulation-specific chitin deacetylase-encoding genes are required for the ascospore wall rigidity of *Saccharomyces cerevisiae*. J. Biol. Chem. 271: 31420–31425.

Christodoulidou, A., P. Briza, A. Ellinger, and V. Bouriotis, 1999 Yeast ascospore wall assembly requires two chitin deacetylase isozymes. FEBS Lett. 460: 275–279.

Chuang, J. S., and R. W. Schekman, 1996 Differential trafficking and timed localization of two chitin synthase proteins, Chs2p and Chs3p. J. Cell Biol. 135: 597–610.

Coluccio, A., E. Bogengruber, M. N. Conrad, M. E. Dresser, P. Briza et al., 2004 Morphogenetic pathway of spore wall assembly in Saccharomyces cerevisiae. Eukaryot. Cell 3: 1464–1475.

Coluccio, A. E., R. K. Rodriguez, M. J. Kernan, and A. M. Neiman, 2008 The yeast spore wall enables spores to survive passage through the digestive tract of Drosophila. PLoS One 3: e2873.

Currie, E., X. Guo, R. Christiano, C. Chitraju, N. Kory et al., 2014 High confidence proteomic analysis of yeast LDs identifies additional droplet proteins and reveals connections to dolichol synthesis and sterol acetylation. J. Lipid Res. 55: 1465–1477.

DeMarini, D. J., A. E. Adams, H. Fares, C. De Virgilio, G. Valle et al., 1997 A septin-based hierarchy of proteins required for localized deposition of chitin in the Saccharomyces cerevisiae cell wall. J. Cell Biol. 139: 75–93.

Deutschbauer, A. M., R. M. Williams, A. M. Chu, and R. W. Davis, 2002 Parallel phenotypic analysis of sporulation and postgermination growth in Saccharomyces cerevisiae. Proc. Natl. Acad. Sci. USA 99: 15530–15535.

Diamond, A. E., J.-S. Park, I. Inoue, H. Tachikawa, and A. M. Neiman, 2009 The anaphase promoting complex targeting subunit Ama1 links meiotic exit to cytokinesis during sporulation in Saccharomyces cerevisiae. Mol. Biol. Cell 20: 134–145.

Enyenihi, A. H., and W. S. Saunders, 2003 Large-scale functional genomic analysis of sporulation and meiosis in Saccharomyces cerevisiae. Genetics 163: 47–54.

Giaever, G., A. M. Chu, L. Ni, C. Connelly, L. Riles et al., 2002 Functional profiling of the Saccharomyces cerevisiae genome. Nature 418: 387–391.

Gibson, D. G., L. Young, R. Y. Chuang, J. C. Venter, C. A. Hutchison, III et al., 2009 Enzymatic assembly of DNA molecules up to several hundred kilobases. Nat. Methods 6: 343–345.

Gohlke, S., S. Muthukrishnan, and H. Merzendorfer, 2017 In vitro and in vivo studies on the structural organization of Chs3 from Saccharomyces cerevisiae. Int. J. Mol. Sci. 18: 702.

Grabińska, K., G. Sosińska, E. Orłowski, E. Swiezewska, T. Berges et al., 2005 Functional relationships between the Saccharomyces cerevisiae cis-prenyltransferases required for dolichol biosynthesis. Acta Biochim. Pol. 52: 221–232.

Grabińska, K. A., J. Cui, A. Chatterjee, Z. Guan, C. R. Raetz et al., 2010 Molecular characterization of the cis-prenyltransferase of Giardia lamblia. Glycobiology 20: 824–832.

Grabińska, K. A., E. J. Park, and W. C. Sessa, 2016 cis-Prenyltransferase: new insights into protein glycosylation, rubber synthesis, and human diseases. J. Biol. Chem. 291: 18582–18590.

Guan, Z., and J. Eichler, 2011 Liquid chromatography/tandem mass spectrometry of dolichols and polyprenols, lipid sugar carriers across evolution. Biochim. Biophys. Acta 1811: 800–806.

Horst, M. N., 1983 The biosynthesis of crustacean chitin. Isolation and characterization of polyprenol-linked intermediates from brine shrimp microsomes. Arch. Biochem. Biophys. 223: 254–263.

Hsu, T. H., R. H. Chen, Y. H. Cheng, and C. W. Wang, 2017 Lipid droplets are central organelles for meiosis II progression during yeast sporulation. Mol. Biol. Cell 28: 440–451.

Iwamoto, M. A., S. R. Fairclough, S. A. Rudge, and J. Engebrecht, 2005 Saccharomyces cerevisiae Sps1p regulates trafficking of enzymes required for spore wall synthesis. Eukaryot. Cell 4: 536–544.

Jin, L., K. Zhang, R. Sternglanz, and A. M. Neiman, 2017 Predicted RNA binding proteins Pes4 and Mip6 regulate mRNA levels, translation, and localization during sporulation in budding yeast. Mol. Cell. Biol. 37: e00408–16.

Jones, M. B., J. N. Rosenberg, M. J. Betenbaugh, and S. S. Krag, 2009 Structure and synthesis of polyisoprenoids used in N-glycosylation across the three domains of life. Biochim. Biophys. Acta 1790: 485–494.

Knop, M., K. Siegers, G. Pereira, W. Zachariae, B. Winsor et al., 1999 Epitope tagging of yeast genes using a PCR-based strategy: more tags and improved practical routines. Yeast 15: 963–972.

Kohlwein, S. D., M. Veenhuis, and I. J. van der Klei, 2013 Lipid droplets and peroxisomes: key players in cellular lipid homeostasis or a matter of fat—store 'em up or burn 'em down. Genetics 193: 1–50.

Kozubowski, L., H. Panek, A. Rosenthal, A. Bloecher, D. J. DeMarini et al., 2003 A Bni4-Glc7 phosphatase complex that recruits chitin synthase to the site of bud emergence. Mol. Biol. Cell 14: 26–39.

Kreger-Van Rij, N. J., 1978 Electron microscopy of germinating ascospores of Saccharomyces cerevisiae. Arch. Microbiol. 117: 73–77.

Kwon, M., E. J. Kwon, and D. K. Ro, 2016 cis-Prenyltransferase and polymer analysis from a natural rubber perspective. Methods Enzymol. 576: 121–145.

Lam, C., E. Santore, E. Lavoie, L. Needleman, N. Fiacco et al., 2014 A visual screen of protein localization during sporulation identifies new components of prospore membrane-associated complexes in budding yeast. Eukaryot. Cell 13: 383–391.

Liang, P.-H., T.-P. Ko, and A. H.-J. Wang, 2002 Structure, mechanism and function of prenyltransferases. Eur. J. Biochem. 269: 3339–3354.

Lin, C. P.-C., C. Kim, S. O. Smith, and A. M. Neiman, 2013 A highly redundant gene network controls assembly of the outer spore wall in S. cerevisiae. PLoS Genet. 9: e1003700.

Loibl, M., and S. Strahl, 2013 Protein O-mannosylation: what we have learned from baker's yeast. Biochim. Biophys. Acta 1833: 2438–2446.

Longtine, M. S., A. McKenzie, III, D. J. Demarini, N. G. Shah, A. Wach et al., 1998 Additional modules for versatile and economical PCR-based gene deletion and modification in Saccharomyces cerevisiae. Yeast 14: 953–961.

Lucero, H. A., M. J. Kuranda, and D. A. Bulik, 2002 A nonradioactive, high throughput assay for chitin synthase activity. Anal. Biochem. 305: 97–105.

Lynn, R. R., and P. T. Magee, 1970 Development of the spore wall during ascospore formation in Saccharomyces cerevisiae. J. Cell Biol. 44: 688–692.

Marston, A. L., W. H. Tham, H. Shah, and A. Amon, 2004 A genome-wide screen identifies genes required for centromeric cohesion. Science 303: 1367–1370.

Mishra, C., C. E. Semino, K. J. McCreath, H. de la Vega, B. J. Jones et al., 1997 Cloning and expression of two chitin deacetylase genes of Saccharomyces cerevisiae. Yeast 13: 327–336.

Morgan, J. L., J. Strumillo, and J. Zimmer, 2013 Crystallographic snapshot of cellulose synthesis and membrane translocation. Nature 493: 181–186.

Neiman, A., 1998 Prospore membrane formation defines a developmentally regulated branch of the secretory pathway in yeast. J. Cell Biol. 140: 29–37.

Neiman, A. M., 2011 Sporulation in the budding yeast Saccharomyces cerevisiae. Genetics 189: 737–765.

Neiman, A. M., L. Katz, and P. J. Brennwald, 2000 Identification of domains required for developmentally regulated SNARE function. Genetics 155: 1643–1655.

Ono, N., T. Yabe, M. Sudoh, T. Nakajima, T. Yamada-Okabe et al., 2000 The yeast Chs4 protein stimulates the trypsin-sensitive activity of chitin synthase 3 through an apparent protein-protein interaction. Microbiology 146: 385–391.

Pammer, M., P. Briza, A. Ellinger, T. Schuster, R. Stucka et al., 1992 DIT101 (CSD2, CAL1), a cell cycle-regulated yeast gene

required for synthesis of chitin in cell walls and chitosan in spore walls. Yeast 8: 1089–1099.

Pan, J. J., L. W. Yang, and P. H. Liang, 2000 Effect of site-directed mutagenesis of the conserved aspartate and glutamate on *E. coli* undecaprenyl pyrophosphate synthase catalysis. Biochemistry 39: 13856–13861.

Park, E. J., K. A. Grabińska, Z. Guan, V. Stránecky, H. Hartmannová *et al.*, 2014 Mutation of Nogo-B receptor, a subunit of *cis*-prenyltransferase, causes a congenital disorder of glycosylation. Cell Metab. 20: 448–457.

Perez, C., S. Gerber, J. Boileven, M. Bucher, T. Darbre *et al.*, 2015 Structure and mechanism of an active lipid-linked oligosaccharide flippase. Nature 524: 433–438.

Ren, J., C. Pei-Chen Lin, M. C. Pathak, B. R. S. Temple, A. H. Nile *et al.*, 2014 A phosphatidylinositol transfer protein integrates phosphoinositide signaling with lipid droplet metabolism to regulate a developmental program of nutrient stress-induced membrane biogenesis. Mol. Biol. Cell 25: 712–727.

Rose, M. D., F. Winston, and P. Hieter, 1990 *Methods in Yeast Genetics: A Cold Spring Harbor Laboratory Course Manual*. Cold Spring Harbor Laboratory Press, Cold Spring Harbor, NY.

Sanyal, S., and A. K. Menon, 2010 Stereoselective transbilayer translocation of mannosyl phophoryl dolichol by an endoplasmic reticulum flippase. Proc. Natl. Acad. Sci. USA 107: 11289–11294.

Sanz, M., J. A. Trilla, A. Duran, and C. Roncero, 2002 Control of chitin synthesis through Shc1p, a functional homologue of Chs4p specifically induced during sporulation. Mol. Microbiol. 43: 1183–1195.

Sato, M., K. Sato, S. Nishikawa, A. Hirata, J. Kato *et al.*, 1999 The yeast *RER2* gene, identified by endoplasmic reticulum protein localization mutations, encodes *cis*-prenyltransferase, a key enzyme in dolichol synthesis. Mol. Cell. Biol. 19: 471–483.

Sato, M., S. Fujisaki, K. Sato, Y. Nishimura, and A. Nakano, 2001 Yeast *Saccharomyces cerevisiae* has two *cis*-prenyltransferases with different properties and localizations. Implication for their distinct physiological roles in dolichol synthesis. Genes Cells 6: 495–506.

Schenk, B., J. S. Rush, C. J. Waechter, and M. Aebi, 2001 An alternative *cis*-isoprenyltransferase activity in yeast that produces polyisoprenols with chain lengths similar to mammalian dolichols. Glycobiology 11: 89–98.

Shaw, J. A., P. C. Mol, B. Bowers, S. J. Silverman, M. H. Valdivieso *et al.*, 1991 The function of chitin synthases 2 and 3 in the *Saccharomyces cerevisiae* cell cycle. J. Cell Biol. 114: 111–123.

Sikorski, R. S., and P. Hieter, 1989 A system of shuttle vectors and yeast host strains designed for efficient manipulation of DNA in *Saccharomyces cerevisiae*. Genetics 122: 19–27.

Smits, G. J., H. van den Ende, and F. M. Klis, 2001 Differential regulation of cell wall biogenesis during growth and development in yeast. Microbiology 147: 781–794.

Suda, Y., H. Nakanishi, E. M. Mathieson, and A. M. Neiman, 2007 Alternative modes of organellar segregation during sporulation in *Saccharomyces cerevisiae*. Eukaryot. Cell 6: 2009–2017.

Swiezewska, E., and W. Danikiewicz, 2005 Polyisoprenoids: structure, biosynthesis and function. Prog. Lipid Res. 44: 235–258.

Szkopińska, A., K. Grabińska, D. Delourme, F. Karst, J. Rytka *et al.*, 1997 Polyprenol formation in the yeast *Saccharomyces cerevisiae*: effect of farnesyl diphosphate synthase overexpression. J. Lipid Res. 38: 962–968.

Tachikawa, H., A. Bloecher, K. Tatchell, and A. M. Neiman, 2001 A Gip1p-Glc7p phosphatase complex regulates septin organization and spore wall formation. J. Cell Biol. 155: 797–808.

Valtersson, C., G. van Duyn, A. J. Verkleij, T. Chojnacki, B. de Kruijff *et al.*, 1985 The influence of dolichol, dolichol esters, and dolichyl phosphate on phospholipid polymorphism and fluidity in model membranes. J. Biol. Chem. 260: 2742–2751.

Wang, C. W., 2015 Lipid droplet dynamics in budding yeast. Cell. Mol. Life Sci. 72: 2677–2695.

Woltering, D., B. Baumgartner, S. Bagchi, B. Larkin, J. Loidl *et al.*, 2000 Meiotic segregation, synapsis, and recombination checkpoint functions require physical interaction between the chromosomal proteins Red1p and Hop1p. Mol. Cell. Biol. 20: 6646–6658.

Yang, H. J., C. L. Hsu, J. Y. Yang, and W. Y. Yang, 2012 Monodansylpentane as a blue-fluorescent lipid-droplet marker for multicolor live-cell imaging. PLoS One 7: e32693.

Yu, L., L. Pena Castillo, S. Mnaimneh, T. R. Hughes, and G. W. Brown, 2006 A survey of essential gene function in the yeast cell division cycle. Mol. Biol. Cell 17: 4736–4747.

Communicating editor: J. Heitman